Journal of Alloys and Compounds 509 (2011) 10127–10131

Contents lists available at SciVerse ScienceDirect

Journal of Alloys and Compounds

journal homepage: www.elsevier.com/locate/jallcom

Influence of surfactants on co-precipitation synthesis of strontium ferrite

H.F. Lu [a], R.Y. Hong [a,b,*], H.Z. Li [b]

[a] College of Chemistry, Chemical Engineering & Materials Science, and Key Laboratory of Organic Synthesis of Jiangsu Province, Soochow University, SIP, Suzhou 215123, China
[b] State Key Laboratory of Multi-phase Complex Systems, Institute of Process Engineering, Chinese Academy of Sciences, Beijing 100080, China

ARTICLE INFO

Article history:
Received 9 April 2010
Received in revised form 10 August 2011
Accepted 14 August 2011
Available online 22 August 2011

Keywords:
Strontium ferrite
Co-precipitation
Surfactant

ABSTRACT

Strontium ferrite ($SrFe_{12}O_{19}$) particles were prepared by co-precipitation method. The ferrite precursors were produced from aqueous mixtures of ferric chloride and strontium nitrate by co-precipitation, using 3 mol/L sodium hydroxide aqueous solutions as precipitant. Three surfactants sodium dodecyl sulfate (SDS), polyethylene glycol 6000 (PEG-6000), cetyltrimethylammonium bromide (CTAB), were applied and the influence of surfactants on the properties of the strontium ferrite particles was studied. The ferrite precursors were first precalcined in a muffle furnace at 400 °C and then mixed with KCl and NaCl using a planetary milling machine in order to lower the calcination temperature. Subsequently the mixtures were calcined at various temperatures. Structure and magnetic properties of the particles were characterized by X-ray powder diffraction, transmission electron microscopy and vibrating sample magnetometer. In this paper, effects of Fe^{3+}/Sr^{2+} mole ratio were first verified and annealing temperatures were then discussed. The results show the strontium ferrite phase begins to form at 650 °C and complete at 800 °C after calcination, and the particles prepared using CTAB exhibit the best properties with respect to particle size and dispersibility.

1. Introduction

Nanoparticles have received increasing attention recently due to their unusual properties, while the interest in hard magnetic materials is growing because of the various technological applications in microwave devices, high-density magnetic recording, electronic devices and medical instruments [1–4]. The remanence M_r for permanent magnet application is a strong function to both physical and chemical properties of ferrite itself while the coercivity mainly originates from its high magnetocrystalline anisotropy and relies on particle microstructure. The properties of this magnetic material depend on the purity, size and morphology of the precursor powder [5]. Thus obtaining fine, high chemical homogeneity and monodispersed particles is the most important process in material manufacturing.

A variety of techniques have been used to prepare strontium ferrite ($SrFe_{12}O_{19}$) of nano-scale including co-precipitation method [6–10], sol–gel process [11–13], glass crystallization [14], the mechanical alloying method [15–17], self-propagation [18,19], microemulsion [20], microwave [21–23], hydrothermal [24] and ultrasound-assisted synthesis [25]. Among them, the co-precipitation is one of the conventional and inexpensive methods to synthesize the strontium ferrite. During co-precipitation, precipitates are generated simultaneously and uniformly dispersed throughout the solution. To obtain the ferrite powder, the precursor must be calcined at high temperatures (≥600 °C) which might lead to some disadvantages including chemical inhomogeneity, coarser particle size and agglomeration. To prevent the above disadvantages, generally surfactants are employed. Although many researchers have investigated the influence of surfactants on the properties of nanoparticles [26–31], studies on preparation of strontium ferrite particles using co-precipitation method have been rarely seen.

In this study, strontium ferrite particles were prepared by co-precipitation. The precursor was precalcined at 400 °C and the molten salt method was applied. Using anionic surfactant (SDS), nonionic surfactant (PEG-6000) and cationic surfactant (CTAB), the influence of surfactants on the properties of the particles were investigated.

2. Experimental procedure

2.1. Materials

Analytical grade ferric chloride ($FeCl_3{\cdot}6H_2O$), strontium nitrate ($Sr(NO_3)_2$), sodium hydroxide (NaOH), polyethylene glycol 6000 (PEG-6000), sodium dodecyl sulfate (SDS), cetyltrimethylammonium bromide (CTAB), ethanol and other materials were used as starting materials. 3 mol/L sodium hydroxide aqueous solutions were used as precipitant. Deionized water was used throughout the experiments.

* Corresponding author at: College of Chemistry, Chemical Engineering & Materials Science, and Key Laboratory of Organic Synthesis of Jiangsu Province, Soochow University, SIP, Suzhou 215123, China. Tel.: +86 512 6588 2057; fax: +86 512 6588 2057.
E-mail address: rhong@suda.edu.cn (R.Y. Hong).

0925-8388/$ – see front matter © 2011 Elsevier B.V. All rights reserved.
doi:10.1016/j.jallcom.2011.08.058

2.2. Particle preparation

The co-precipitation method was applied for the preparation of nano-strontium ferrite ($SrFe_{12}O_{19}$). $FeCl_3{\cdot}6H_2O$ and $Sr(NO_3)_2$ were dissolved in 50 ml of deionized water with a molar ratio of 1:9.23, which was proposed by Hessien et al. [10] as the best ratio. Different kinds of surfactants of 1 wt% amount were added into the above saline mixture solution to avoid agglomeration during calcination. Such solution was added dropwise into the sodium hydroxide aqueous to form the homogeneous precursor. Meanwhile, in order to maintain the pH of the reaction solution (pH 11), extra sodium hydroxide aqueous with same concentration was added to compensate the consumed one. The whole reaction was carried out under vigorous stirring at 80 °C in a water bath. The aqueous suspension was stirred gently for another 30 min and then cooled in water under room temperature immediately. Reddish brown co-precipitate was washed by deionized water for 5 times and ethanol for 3 times, respectively. The co-precipitant was centrifuged for 10 min to remove ethanol, and then dried at 100 °C overnight. The as-dried particles were precalcined in air at 400 °C for 2 h.

The obtained oxide mixtures were then mixed with an equimolar mixture of NaCl and KCl, using alcohol as medium. The mixture was milled with a planetary milling machine operating at the speed of 40 rpm for 2 h and dried later. The mixed sample was calcined in a muffle furnace at various temperatures from 600 to 1000 °C for 2 h in air, and then cooled to room temperature. The product was washed several times with deionized water and alcohol to remove the impurities, and centrifuged, then dried in an oven at 100 °C.

2.3. Characterization

The size of the strontium ferrite nanoparticles was determined from transmission electron microscopy (TEM) images using H-600-II transmission electron microscope (Hitachi, Japan) and from analysis of the broadened major peak of XRD spectra. Magnetic properties of strontium ferrite nanoparticles were measured using a BHV-55 vibrating sample magnetometer (VSM).

3. Results and discussion

Different kinds of dispersants such as anionic surfactant (SDS), cationic surfactant (CTAB) and nonionic surfactant (PEG-6000) were used to reduce the size of the aggregates and improve the dispersibility of the strontium ferrite nanoparticles. Three samples named as S1, S2 and S3 were prepared using surfactants SDS, CTAB, PEG-6000 respectively while sample S0 represented the one without surfactant.

3.1. XRD analysis of strontium ferrite particles

To monitor the formation of the crystalline phase with increasing calcination temperature, the as-dried precursors obtained by co-precipitation were calcined for 2 h in air at different temperatures, up to 1000 °C. Then the phase transformation is analyzed by comparing XRD patterns. Fig. 1 shows the X-ray diffraction patterns of sample S0 derived from co-precipitation at various temperatures

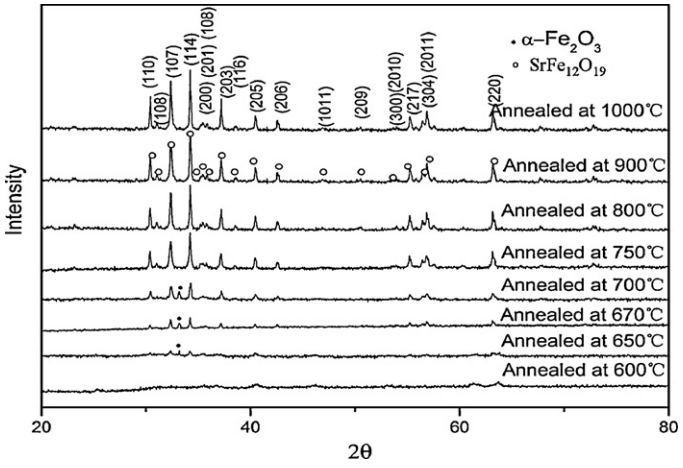

Fig. 1. XRD patterns of sample S0 annealed at temperatures from 600 to 1000 °C for 2 h.

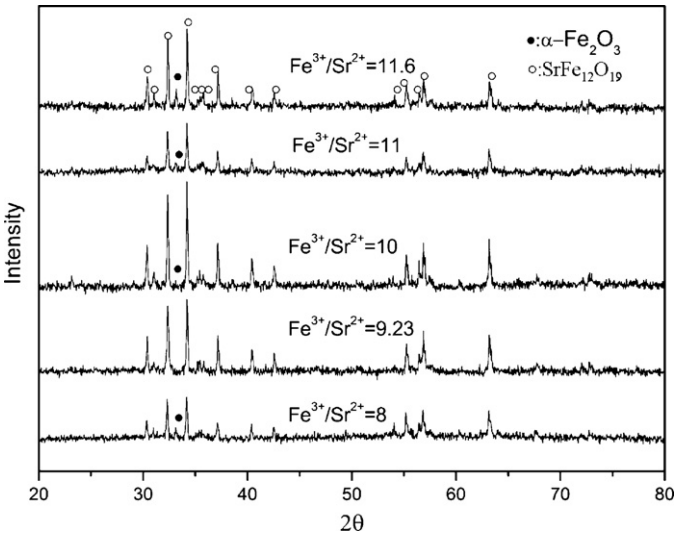

Fig. 2. XRD patterns of sample S0 annealed at different Fe^{3+}/Sr^{2+} ratio under 800 °C.

ranging from 600 to 1000 °C for annealing time 2 h. It is found that heating the precursor at a rate of 10 °C/min to 600 °C resulted in a remained amorphous state. While calcined at temperature 650 °C, small amount of $SrFe_{12}O_{19}$ crystal phase transitions are identified, which is indicated by the appearance of (1 0 7) and (1 1 4) peaks at 2θ angles of 32.343° and 34.191°, respectively. It is evident that particles calcined below 700 °C contain some peaks of impurity (α-Fe_2O_3 phase), which may be probably due to the occurrence of local calcination. As the calcination temperature increases, the identified peaks of strontium phase appear while the peaks of α-Fe_2O_3 phase disappear. It is worth noting that the peaks of α-Fe_2O_3 phase are weak because of the small amount, tiny particle size and homogeneity of the precursor and the employ of molten salt method.

When the temperature reaches 800 °C, a well-crystallized pure strontium ferrite phase is formed. The sample gives sharp XRD peaks, and all the prominent peaks (1 1 0), (1 0 8), (1 0 7), (1 1 4), (2 0 0), (2 0 1), (1 0 8), (2 0 3), (1 1 6), (2 0 5), (2 0 6), (1 0 1 1), (2 0 9), (3 0 0), (2 0 1 0), (2 1 7), (3 0 4), (2 0 1 1) and (2 2 0) are observed at the corresponding angles in the peak positions, which is in excellent accordance with the powder data of index card JCPDS-ICDD number 84-1531. When the annealing temperature exceeds 900 °C, the crystalline of $SrFe_{12}O_{19}$ is further enhanced as expected while the particle size would increase due to agglomeration. The comparison of several experiments using different ratios of metal ions after calcination at 800 °C is displayed in Fig. 2, demonstrating the reliability of the work of Hessien et al. [10].

The X-ray diffraction patterns of sample S0–S4 annealed at 800 °C for 2 h are shown in Fig. 3, which indicates the fact that surfactant can be used to improve the dispersibility and enhance the formation of single phase ferrite at low calcination temperature. The crystallite sizes, as shown in Table 1, are calculated using the X-ray broadening of the (1 1 4) diffraction peak by the well-known Scherrer equation: $D = 0.9\lambda/(\beta\cos\theta)$, where D is the particle size in nm, λ the wavelength of the X-ray (0.15405 nm for Cu-Ka), β the corrected full width at half maximum and θ is the diffraction angle.

Table 1
Comparison of crystallite sizes obtained by XRD and TEM measurement.

Sample	XRD (nm)	TEM (nm)
S0	40	45
S1	38	50
S2	30	35
S3	37	40

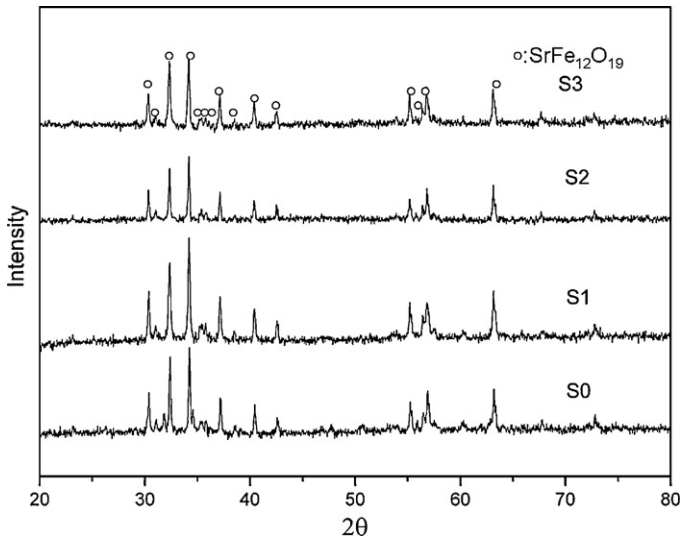

Fig. 3. XRD patterns of samples S0–S4 annealed at 800 °C for 2 h.

3.2. TEM analysis of strontium ferrite particles

The micrographs of S0, S1, S2 and S3 (annealed at 800 °C) are shown in Fig. 4(a)–(d), respectively. Severe aggregation of sample S0 with particle size of about 45 nm is shown in Fig. 4(a) while in Fig. 4(b)–(d), particles with very slight aggregation can be observed, which are composed of irregular fine particles. The average size of particles is about 50, 35 and 40 nm, respectively, which is accordance with the XRD analysis. Table 1 lists the results from XRD and TEM analysis. From the table, it is clear that the particles sizes observed from TEM micrographs are larger than that calculated from XRD analysis and the sample with more serious aggregation leads generally to larger difference between XRD and TEM measurements.

According to the comparison in Table 1, it is clear that the addition of surfactants leads generally to smaller size particles, which is due to the stabilization properties and steric hindrance of surfactants. The surfactants are absorbed on the surface of the precipitant to prevent agglomeration of the hydroxide precipitation by bridging bond of hydroxyl. As a result of addition of different kinds of surfactants during the co-precipitation, the obtained particles exhibit different degree aggregation. The size of particles prepared with CTAB surfactant is the smallest, PEG-6000 is moderate and SDS is the poorest among three, which may be attributed to different kinds of charge possessed by surfactants. The precipitates possess negative charge with the excess of hydroxyl at the aqueous solution (pH 11), therefore those cationic surfactants such as CTAB can be absorbed on the surface of the precipitate particles much easier and form a molecular film on the surface of the particles to keep them away from aggregation. Macromolecular surfactants (such as PEG) can play a certain steric hindrance effect. There are two kinds of hydrophilic groups (hydroxyl group and ether linkage) in PEG molecule, so the PEG is a good water soluble surfactant. In aqueous solution, the molecule of PEG looks like a snake, so it can easily be adsorbed on the surface of the particles to form a macromolecule protection layer. Due to the dimensional hindrance effect of PEG, precipitate particles with smaller size can be obtained. For anionic surfactant SDS, the repulsive force leads to poor absorption and aggregation.

3.3. VSM analysis of strontium ferrite particles

The magnetic properties of the strontium ferrite nanoparticles are measured by VSM. Results of which are shown in Fig. 5, (a)

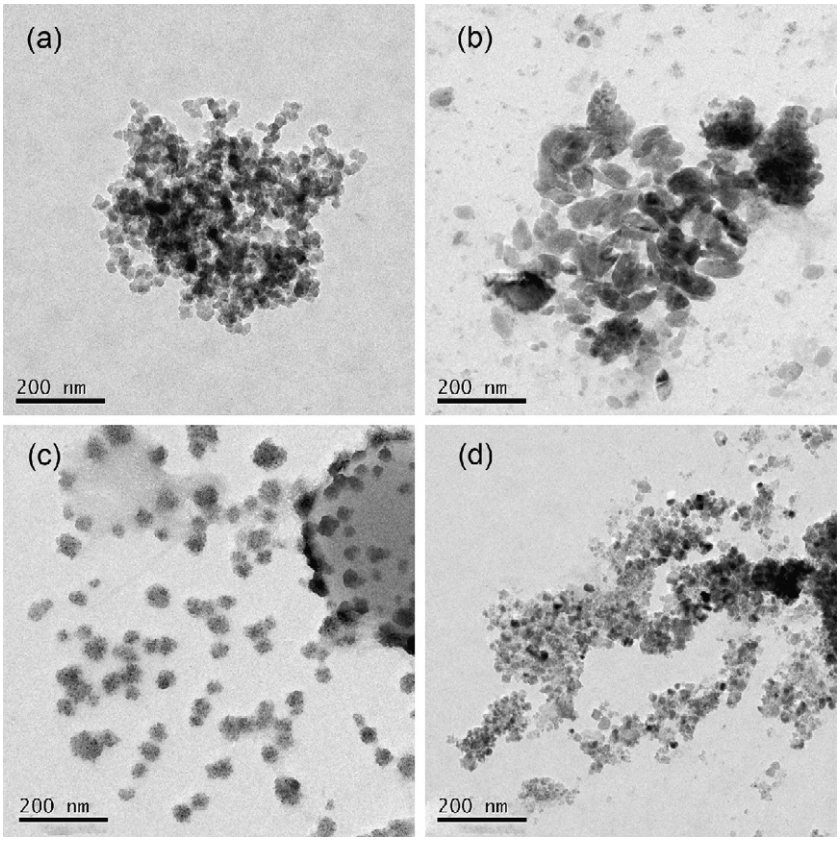

Fig. 4. TEM images of $SrFe_{12}O_{16}$ powders: (a) without surfactant, (b) SDS as surfactant, (c) CTAB as surfactant, (d) PEG-6000 as surfactant.

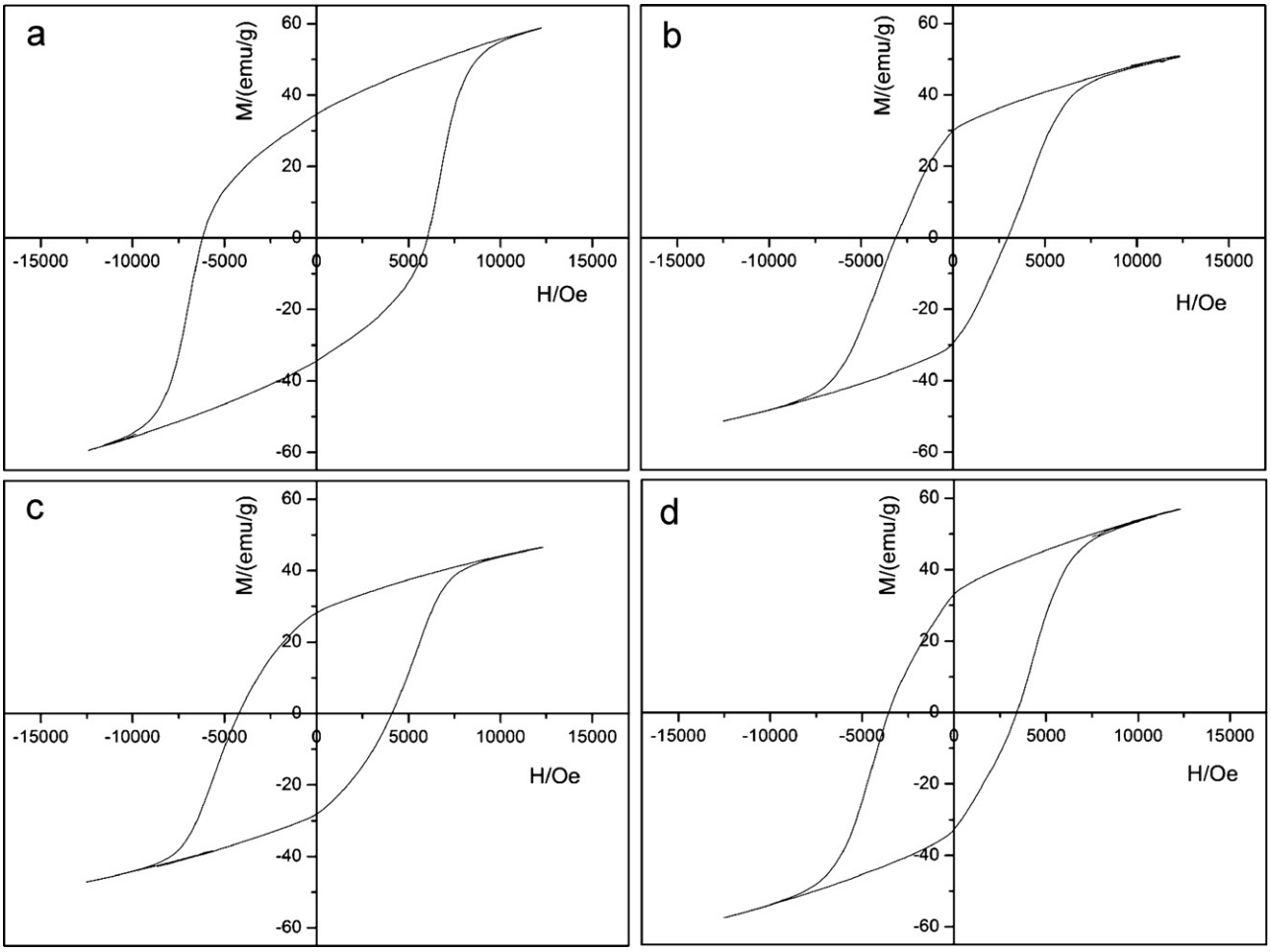

Fig. 5. Magnetic hysteresis of $SrFe_{12}O_{16}$ annealed at 800 °C: (a) without surfactant, (b) SDS as surfactant, (c) CTAB as surfactant (d) PEG-6000 as surfactant.

Table 2
Intrinsic coercive force (H_c) and the saturation magnetization (M_s).

Sample	H_c (Oe)	M_s (emu/g)
S0	6031	58.9
S1	2966	51.0
S2	4099	46.5
S3	3411	56.9

strontium ferrite particles without surfactant, (b) SDS, (c) CTAB, (d) PEG-6000. The intrinsic coercive force (H_c) and the saturation magnetization (M_s) are shown in Table 2. From Table 2 and Fig. 5, it is clear that adding surfactants may lead to the decrease of H_c and M_s, which can be attributed to surface effects such as magnetically inactive layer containing spins that were not collinear with the magnetic field [32,33]. From four magnetic hysteresis curves, it can be found that particles prepared with CTAB exhibit the maximum H_c compared to the samples with SDS and PEG. From Table 2, it is found that the M_s of the sample S2 is smaller than that of S1 and S3. This result can be ascribed to the fact that the particle of S2 is smaller than S1 and S3.

4. Conclusions

Using strontium nitrate ($Sr(NO_3)_2$), ferric chloride ($FeCl_3{\cdot}6H_2O$), sodium hydroxide (NaOH), polyethylene glycol 6000 (PEG-6000), sodium dodecyl sulfate (SDS), cetyltrimethylammonium bromide (CTAB), and ethanol as the starting materials, well dispersed strontium ferrite powders have been synthesized successfully by co-precipitation. Results show that the application of surfactants and molten salt method decrease the calcination temperature. The strontium ferrite phase begins to form at 650 °C and complete at 800 °C after annealing time 2 h. Different kinds of surfactants such as anionic surfactant (SDS), nonionic surfactant (PEG-6000) and cationic surfactant (CTAB) are employed to reduce the size and improve the dispersibility of strontium ferrite particles. Results of this study show that the size of particles prepared with CTAB surfactant is the smallest, PEG-6000 is moderate and SDS is the poorest among three. Both XRD and TEM reveal the obtained particle is about 35–50 nm in size and well dispersed. All results show that particles prepared using CTAB as surfactant exhibit the best properties with respect to particle size and dispersibility.

Acknowledgements

The project was supported by the National Natural Science Foundation of China (NSFC, nos. 20876100 and 20736004), the National Basic Research Program of China (973 Program, no. 2009CB219904), the State Key Lab. of Multiphase Complex Systems of the Chinese Academy of Science (no. 2006-5), the Key Lab. of Organic Synthesis of Jiangsu Prov., R&D Foundation of Nanjing Medical Univ. (NY0586), Post-doctoral Science Foundation of Jiangsu Prov., National Post-doctoral Science Foundation (20090451176), and the Commission of Science and Technology of Suzhou Municipality, China (YJS0917, SG0978).

References

[1] M.H. Sousa, F.A. Tourinho, J. Depeyrot, G.J. da Silva, M.C.F.L. Lara, J. Phys. Chem. B 105 (2001) 1168–1175.
[2] S.R. Mekala, J. Ding, J. Alloys Compd. 296 (2000) 152–156.
[3] S.E. Jacobo, L. Civale, M.A. Blesa, J. Magn. Magn. Mater. 260 (2000) 37–41.
[4] Y.F. Lu, W.D. Song, Appl. Phys. Lett. 76 (2000) 490–492.
[5] X. Sui, M. Scherge, M.H. Kryder, J.E. Snyder, V.G. Harris, N.C. Koon, J. Magn. Magn. Mater. 155 (1996) 132–139.
[6] D.H. Chen, Y.Y. Chen, Mater. Res. Bull. 37 (2002) 801–810.
[7] A. Ataie, S. Heshmati-Manesh, J. Eur. Ceram. Soc. 21 (2001) 1951–1955.
[8] V. Uskoković1, D. Makovec, M. Drofenik, Mater. Sci. Forum 494 (2005) 155–160.
[9] Z.F. Zi, Y.P. Sun, X.B. Zhu, Z.R. Yang, J.M. dai, W.H. Song, J. Magn. Magn. Mater. 320 (2008) 2746–2751.
[10] M.M. Hessien, M.M. Rashad, K. El-Barawy, J. Magn. Magn. Mater. 320 (2008) 336–343.
[11] A. Ghasemi, A. Morisako, X. Liu, J. Magn. Magn. Mater. 320 (2008) 2300–2304.
[12] Y. Wang, Q. Li, C. Zhang, H. Jing, J. Alloys Compd. 467 (2009) 284–287.
[13] Y. Wang, Q. Li, C. Zhang, B. Li, J. Magn. Magn. Mater. 321 (2009) 3368–3372.
[14] H. Sato, T. Umeda, J. Mater. Trans. 34 (1993) 76–81.
[15] J. Ding, W.F. Miao, P.G. McCormick, R. Street, J. Alloys Compd. 281 (1998) 32–36.
[16] W.A. Kaczmarek, B. Idzikowski, K.H. Muller, J. Magn. Magn. Mater. 177 (1998) 921–922.
[17] S.V. Ketov, Y.D. Yagodkin, A.L. Lebed, Yu.V. Chernopyatova, K. Khlopkov, J. Magn. Magn. Mater. 300 (2006) 479–481.
[18] X. Yang, Q. Li, J. Zhao, B. Li, Y. Wang, J. Alloys Compd. 475 (2009) 312–315.
[19] L. You, L. Qiao, J. Zheng, M. Jiang, L. Jiang, J. Sheng, J. Rare Earth 26 (2008) 81–84.
[20] S. Chaudhury, S.K. Rakshit, S.C. Parida, Z. Singh, K.D.S. Mudhera, V. Venugopal, J. Alloys Compd. 455 (2008) 25–30.
[21] Y.P. Fu, C.H. Lin, K.Y. Pan, J. Alloys Compd. 349 (2003) 228–231.
[22] Y.P. Fu, C.H. Lin, J. Alloys Compd. 386 (2005) 222–227.
[23] F. Tabatabaie, M.H. Fathia, A. Saatchia, A. Ghasemia, J. Alloys Compd. 470 (2009) 332–335.
[24] J.F. Wang, C.B. Ponton, R. Grössinger, I.R. Harris, J. Alloys Compd. 369 (2004) 170–177.
[25] I. Perelshtein, N. Perkas, S. Magdassi, T. Zioni, M. Royz, Z. Maor, A. Gedanken, J. Nanopart. Res. 10 (2008) 191–195.
[26] C.L. Robert, F. Ansart, S. Castillo, G. Richard, Solid State Sci. 4 (2002) 1053–1059.
[27] A.P. Jadhav, C.W. Kim, H.G. Cha, A.U. Pawar, N.A. Jadhav, U. Pal, Y.S. Kang, J. Phys. Chem. C 113 (2009) 13600–13604.
[28] M.G. Hasab, S.A.S. Ebrahimi, A. Badiei, J. Magn. Magn. Mater. 316 (2007) 13–15.
[29] M.G. Hasab, S.A. Seyyed Ebrahimi, A. Badiei, J. Magn. Magn. Mater. 310 (2007) 2477–2479.
[30] A.P.A. Faiyas, E.M. Vinod, J. Joseph, R. Ganesan, R.K. Pandey, J. Magn. Magn. Mater. 322 (2010) 400–404.
[31] M.M. Rashad, M. Radwan, M.M. Hessien, J. Alloys Compd. 453 (2008) 304–308.
[32] M. Yamaura, R.L. Camilo, L.C. Sampaio, M.A. Macedo, M. Nakamura, H.E. Toma, J. Magn. Magn. Mater. 279 (2004) 210–217.
[33] I. Lisiecki, F. Billoudet, M.P. Pileni, J. Phys. Chem. 100 (1996) 4160–4166.